

LETTER TO THE EDITOR

# Detection of extragalactic CF<sup>+</sup> toward PKS 1830–211

## Chemical differentiation in the absorbing gas

S. Muller<sup>1</sup>, K. Kawaguchi<sup>2</sup>, J. H. Black<sup>1</sup>, and T. Amano<sup>3</sup>

<sup>1</sup> Department of Earth and Space Sciences, Chalmers University of Technology, Onsala Space Observatory, 43992 Onsala, Sweden  
e-mail: mullers@chalmers.se

<sup>2</sup> Department of Chemistry, Okayama University, Tsushima-naka 3-1-1, Kitaku, 700-8530 Okayama, Japan

<sup>3</sup> Department of Chemistry and Department of Physics and Astronomy, University of Waterloo, Waterloo, ON N2L 3G1, Canada

Received 11 March 2016 / Accepted 1 April 2016

### ABSTRACT

We report the first extragalactic detection of the fluoromethyldinium ion CF<sup>+</sup> in the  $z = 0.89$  absorber toward PKS 1830–211. We estimate an abundance of  $\sim 3 \times 10^{-10}$  relative to H<sub>2</sub> and that  $\sim 1\%$  of fluorine is captured in CF<sup>+</sup>. The absorption line profile of CF<sup>+</sup> is found to be markedly different from that of other species observed within the same tuning, and is notably anticorrelated with CH<sub>3</sub>OH. On the other hand, the CF<sup>+</sup> profile resembles that of [C I]. Our results are consistent with expected fluorine chemistry and point to chemical differentiation in the column of absorbing gas.

**Key words.** quasars: absorption lines – quasars: individual: PKS1830-211 – galaxies: ISM – galaxies: abundances – ISM: molecules – radio lines: galaxies

## 1. Introduction

The CF<sup>+</sup> molecule was discovered in space by Neufeld et al. (2006) toward the Orion Bar region. It has recently been identified in Galactic diffuse clouds in absorption toward the background continuum sources 3C111, BL Lac, and W49 (Liszt et al. 2014, 2015). It is also detected toward a high-mass protostar (Fechtenbaum et al. 2015) and is therefore a ubiquitous species in the interstellar medium (ISM).

The chemistry of CF<sup>+</sup> and other fluorine-bearing species has been investigated by Neufeld et al. (2005) and Neufeld & Wolfire (2009). With an ionization potential higher than that of hydrogen, fluorine is mostly neutral in the diffuse ISM. In addition, it is a special element in that it has an exothermic reaction with H<sub>2</sub>. With increasing H<sub>2</sub> fractional abundance, HF thus becomes the main interstellar reservoir of fluorine (F+H<sub>2</sub> → HF+H). HF is destroyed by reactions with He<sup>+</sup>, H<sub>3</sub><sup>+</sup>, and C<sup>+</sup>. The latter reaction forms CF<sup>+</sup> (HF+C<sup>+</sup> → CF<sup>+</sup>+H), which is destroyed by dissociative recombination. Eventually, CF<sup>+</sup> is expected to account for a small fraction ( $\sim 1\%$ ; Neufeld & Wolfire 2009) of the gas-phase fluorine.

Recently, H<sub>2</sub>Cl<sup>+</sup> was detected in the  $z = 0.89$  molecular absorber toward the lensed blazar PKS 1830–211 (Muller et al. 2014b), making it a good case to search for other halogen-bearing species. The absorber toward PKS 1830–211 consists in two lines of sight, intercepting the disk of a  $z = 0.89$  face-on spiral galaxy (Wiklind & Combes 1996; Winn et al. 2002). Molecular absorption is seen in both lines of sight with H<sub>2</sub> column density of  $\sim 2 \times 10^{22}$  cm<sup>-2</sup> toward the southwest image of the blazar and  $\sim 1 \times 10^{21}$  cm<sup>-2</sup> toward the northeast image. More than 40 molecules have been detected in the SW line of sight (e.g., Muller et al. 2011, 2014a). The fractional abundances in the absorber are typical of those in-between diffuse and translucent Galactic clouds. Because the density is moderate,

$n(\text{H}_2) \sim 10^3$  cm<sup>-3</sup> toward SW and likely even lower toward NE, the excitation of polar molecules is subthermal and radiatively coupled to the cosmic microwave background (CMB). Hence, their rotation temperature is equal to 5.14 K, i.e., the CMB temperature at  $z = 0.89$  (Muller et al. 2013). As a result, the absorption spectrum toward PKS 1830–211 is not too crowded (only low-energy levels are populated) and line identification is easy.

Here, we report the ALMA detection of CF<sup>+</sup> at  $z = 0.89$  toward PKS 1830–211, which is the first extragalactic detection of this species.

## 2. Observations

The observations of the CF<sup>+</sup>  $J = 2-1$  line, redshifted to 108.8 GHz at  $z_{\text{abs}} = 0.88582$  (heliocentric frame), were taken during the ALMA Early Science Cycle 2 phase on 2014 August 27th. Two execution blocks of six minutes on source were observed. The correlator was configured with four different spectral windows of 1.875 GHz, each counting 3840 channels separated by 0.488 MHz, providing a velocity resolution of  $\sim 2.6$  km s<sup>-1</sup> after Hanning smoothing.

The data calibration was carried out within the CASA<sup>1</sup> package, following a standard procedure. The bandpass response of the antennas was calibrated from observations of the bright quasar J1924–292. The quasar J1832–2039 was used for primary gain calibration. We further improved the data quality using self-calibration on the bright continuum of PKS 1830–211. The spectra were extracted toward both lensed images of PKS 1830–211, using the CASA-python task UVMULTIFIT (Martí-Vidal et al. 2014) to fit a model of two point sources to the visibilities. We note that the two lensed images of

<sup>1</sup> <http://casa.nrao.edu/>

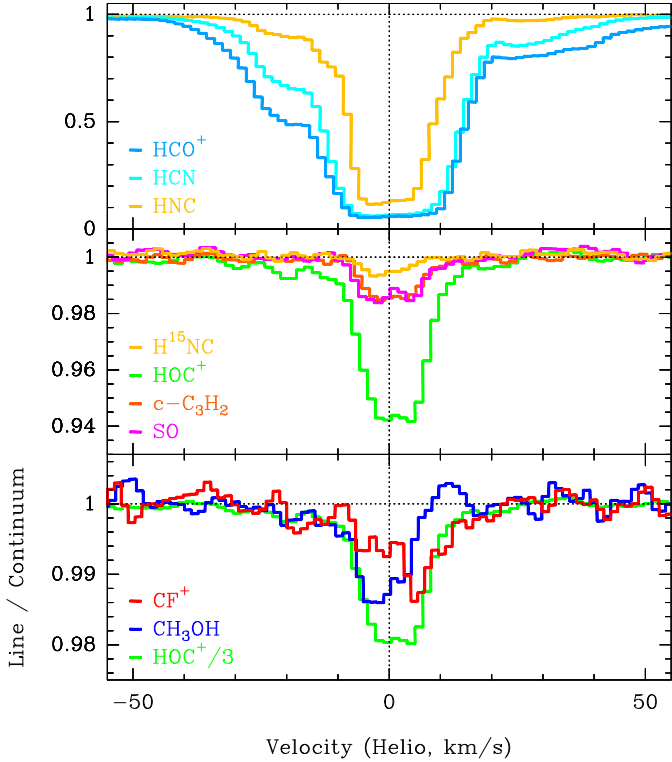


**Fig. 1.** Spectra of  $\text{CF}^+$  and other species observed simultaneously toward the SW image of PKS 1830–211.

PKS 1830–211,  $1''$  apart, were clearly spatially resolved with a synthesized beam of  $0.75'' \times 0.55''$  (Briggs weighting with robust parameter set to 0.5) in the CLEAN-deconvolved maps.

### 3. Results and discussion

The spectrum of  $\text{CF}^+$   $J = 2-1$  toward the SW image of PKS 1830–211 is shown in Fig. 1, together with some other lines observed within the same tuning, namely from  $\text{HCO}^+$ ,  $\text{HCN}$ ,  $\text{HNC}$ ,  $\text{HOC}^+$ ,  $c\text{-C}_3\text{H}_2$ ,  $\text{SO}$ , and  $\text{CH}_3\text{OH}$ . All these lines arise in low-energy levels (see Table 1).  $\text{CF}^+$  is not detected toward the NE image (down to a rms of  $\sim 0.001$  of the continuum level per  $2.6 \text{ km s}^{-1}$  channel), where the absorbing gas is found to be more atomic and diffuse than along the SW line of sight. This confirms that  $\text{CF}^+$  is tracing gas that already has a substantial molecular fraction. We restrict the discussion to the SW line of sight.

Despite having only one transition of  $\text{CF}^+$ , its identification is robust. As we already mentioned, the line crowding toward PKS 1830–211 is low and we could not find any other possible alternative identification, except  $^{13}\text{CN } N = 1-0$  at  $z = 0$ , but we would expect the line to be: 1) very narrow (a few  $\text{km s}^{-1}$ ; see the Galactic absorption of  $c\text{-C}_3\text{H}_2$  toward PKS 1830–211 by Schulz et al. 2015) and decomposed into its characteristic spin-rotation and hyperfine pattern; and 2) very weak, as even the  $\text{HCO}^+/\text{HCN}/\text{C}_2\text{H } J = 1-0$  Galactic absorptions toward PKS 1830–211 are no more than a few percent deep (Muller et al., in prep).

The hyperfine structure in the rotational spectrum of  $\text{CF}^+$  has been explored by Guzmán et al. (2012). For the  $J = 2-1$  transition, the maximum spread between hyperfine components is less than  $1 \text{ km s}^{-1}$  in the rest frame (this spread is to be divided by 1.89 due the redshift of the absorption), i.e., much narrower than the absorption line width ( $\sim 15 \text{ km s}^{-1}$ ; FWHM). We therefore neglect the hyperfine structure splitting in the following.

The continuum source covering factor  $f_c$  can be inferred from the saturation level of the  $\text{HCO}^+$  and  $\text{HCN } J = 2-1$  lines, yielding  $f_c \sim 94\%$ <sup>2</sup>. This is a strong indication that weak absorption of a few percent of the continuum level corresponds to optically thin lines. The  $\text{CF}^+$  absorption, at most  $\sim 1.5\%$  of the continuum level, is thus likely to be optically thin. However, the  $\text{CF}^+$  absorption does not resemble that of any other species observed within the same tuning (Fig. 1). In fact, we can classify the species into four categories depending on their line profiles: 1)  $\text{HCO}^+$ ,  $\text{HCN}$ , and  $\text{HNC}$ , with their optically thick absorption ( $\text{HCO}^+$  and  $\text{HCN}$  reach saturation); 2)  $\text{HOC}^+$ ,  $c\text{-C}_3\text{H}_2$ , and  $\text{SO}$ , which are optically thin and trace the bulk of the main absorption between about  $-20 \text{ km s}^{-1}$ <sup>3</sup> to  $+20 \text{ km s}^{-1}$ ; 3)  $\text{CF}^+$ , which peaks on the red wing at about  $+5 \text{ km s}^{-1}$ , although its absorption is also seen over the main  $-20 \text{ km s}^{-1}$  to  $+20 \text{ km s}^{-1}$  velocity range; and 4)  $\text{CH}_3\text{OH}$ , which peaks on the blue wing at about  $-3 \text{ km s}^{-1}$ .

It is interesting to note that in previous observations toward PKS 1830–211, only few species show slight but significant deviations in their velocity centroids compared to the majority of detected species. In the 7 mm spectral scan obtained with the Australia Telescope Compact Array (ATCA), Muller et al. (2011) found that  $\text{HCO}$  and  $\text{SO}^+$  had a redshifted centroid ( $\sim +4 \text{ km s}^{-1}$ )<sup>4</sup>, similar to  $\text{CF}^+$  here. On the other hand,  $\text{CH}_3\text{OH}$ ,  $\text{HNC}$ ,  $\text{HC}_3\text{N}$ , and  $\text{CH}_3\text{NH}_2$  were found with blueshifted centroids ( $\sim -5 \text{ km s}^{-1}$ ), such as  $\text{CH}_3\text{OH}$  here. A similar centroid was found by Kanekar et al. (2015) on the line profile of several  $\text{CH}_3\text{OH}$  lines observed at good signal-to-noise ratio with the Jansky Very Large Array. The time variations of the absorption (Muller & Guélin 2008; Muller et al. 2014a) hamper the comparison of line profiles across time, but at a given epoch, the relative offsets of the line velocity centroids between different species are meaningful. Since all those lines have similar excitation, the offsets ought to originate from differences in the chemical or physical properties of the absorbing medium. In Fig. 2, we compare the new spectra obtained in 2014 with those of the same lines observed in 2012 (Muller et al. 2014a; ALMA Cycle 0 data). For  $\text{HOC}^+$ , the 2014 spectrum is about 30% deeper around  $v = 0 \text{ km s}^{-1}$  and the blue wing has become slightly less prominent (same as for the  $\text{HCO}^+$  and  $\text{HCN}$  profiles), but overall the line shape has not changed drastically. Most interestingly, of all species observed in 2012 by ALMA,  $[\text{C I}]$  has the closest line profile to  $\text{CF}^+$ . Neutral carbon is naturally expected to be present in regions better shielded and slightly denser than for ionized carbon. Since  $\text{CF}^+$  is produced from  $\text{C}^+$ , we expect an even better correlation between  $\text{CF}^+$  and  $[\text{C II}]$  lines.

By integrating over the line between  $-20 \text{ km s}^{-1}$  to  $+20 \text{ km s}^{-1}$  and assuming thermal equilibrium with CMB photons, we find a total  $\text{CF}^+$  column density of  $5.5 \times 10^{12} \text{ cm}^{-2}$ . With a  $\text{H}_2$  column density of  $2 \times 10^{22} \text{ cm}^{-2}$  (Muller et al. 2014a), this corresponds to an averaged fractional abundance  $[\text{CF}^+]/[\text{H}_2]$  of  $\sim 3 \times 10^{-10}$ . The cosmic abundance of fluorine is a few times  $10^{-8}$  that of hydrogen (Snow et al. 2007; Asplund et al. 2009). Assuming that the fluorine abundance is similar in the absorbing clouds of the  $z = 0.89$  galaxy, we conclude that only  $\sim 1\%$  of the interstellar fluorine is captured in  $\text{CF}^+$  in agreement with predictions from Neufeld & Wolfire (2009). The  $\text{CF}^+$  production and destruction may be expressed

<sup>2</sup> We note that this value is slightly higher than that observed in 2012 ( $\sim 91\%$ ) by Muller et al. (2014a); see Fig. 2.

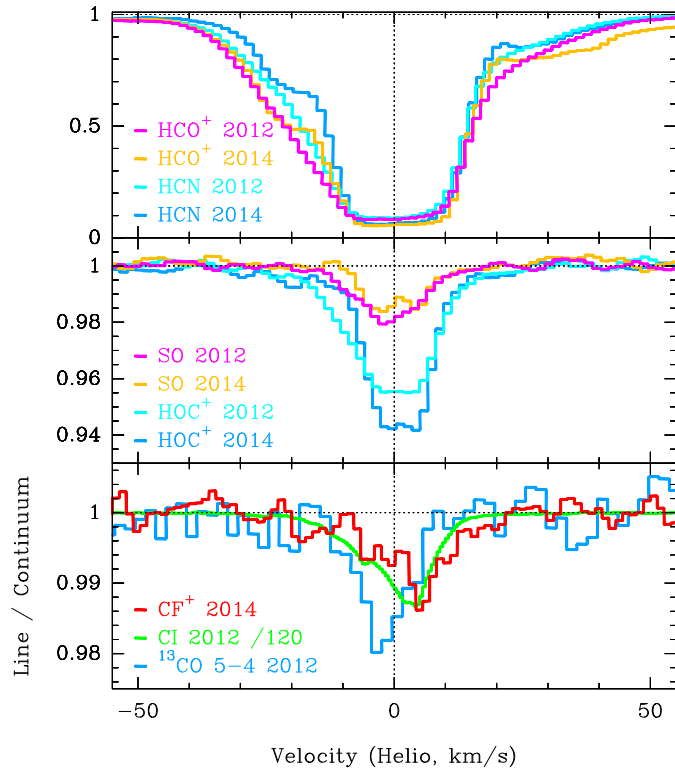
<sup>3</sup> Throughout the paper, we refer the velocity to the heliocentric frame, taking  $z_{\text{abs}} = 0.88582$ .

<sup>4</sup> The velocity resolution of the ATCA 7 mm survey is limited to  $\sim 10\text{--}6 \text{ km s}^{-1}$  across the 30–50 GHz frequency interval.

**Table 1.** List of lines detected at  $z = 0.89$  toward the SW image of PKS 1830–211 and discussed in this paper.

Line	Rest freq. (GHz)	Sky freq. $z = 0.88582$ (GHz)	$E_{\text{low}}^a$ (K)	$S_{\text{ul}}^b$	Dipole moment (Debye)	$\alpha^c$ ( $10^{12} \text{ cm}^{-2} \text{ km}^{-1} \text{ s}$ )	$\int \tau dv^d$ ( $\text{km s}^{-1}$ )	$N_{\text{col}}^e$ ( $10^{12} \text{ cm}^{-2}$ )
HCN (2–1)	177.26111	93.997	4.3	2.0	2.99	3.5	–	–
HCO <sup>+</sup> (2–1)	178.37506	94.588	4.3	2.0	3.90	2.1	–	–
SO (5 <sub>4</sub> –4 <sub>3</sub> )	178.60540	94.710	15.9	4.9	1.54	141.8	0.24	34.0
HOC <sup>+</sup> (2–1)	178.97205	94.904	4.3	2.0	2.77	4.1	1.04	4.3
HNC (2–1)	181.32476	96.152	4.4	2.0	3.05	3.4	41.9	142.5
c-C <sub>3</sub> H <sub>2</sub> ( <i>para</i> ) (4 <sub>1,3</sub> –3 <sub>2,2</sub> )	183.62362	97.371	16.1	2.4	3.43	59.7	0.23	13.7
CF <sup>+</sup> (2–1)	205.17052	108.796	4.9	2.0	1.13	26.2	0.21	5.5
CH <sub>3</sub> OH (1 <sub>1</sub> A <sup>+</sup> –2 <sub>0</sub> A <sup>+</sup> )	205.79127	109.126	7.0	0.5	1.44	255.1	0.18	45.9

**Notes.** Frequencies and molecular data are taken from the Cologne Database for Molecular Spectroscopy (Müller et al. 2001). <sup>(a)</sup>  $E_{\text{low}}$  is the lower level energy of the transition. <sup>(b)</sup>  $S_{\text{ul}}$  is the line strength. <sup>(c)</sup>  $\alpha$  is defined as the conversion factor between integrated opacity and total column density  $N_{\text{col}} = \alpha \times \int \tau dv$ , calculated under the assumption that the rotational excitation is coupled with the cosmic microwave background temperature, 5.14 K at  $z = 0.89$  (see, e.g., Muller et al. 2013). <sup>(d)</sup> Integrated opacity, over the velocity interval  $[-20; +20] \text{ km s}^{-1}$ . The associated uncertainty is of 0.003 at  $1\sigma$ . <sup>(e)</sup> Total column density in the same velocity interval.


**Fig. 2.** Comparison of spectra obtained in 2014 and previous ALMA Cycle 0 spectra observed in 2012.

as follows, in diffuse clouds,



with the formation rate  $k_f = 7.2 \times 10^{-9} \times (T/300)^{-0.15} \text{ cm}^3 \text{ s}^{-1}$ ,  $T$  is the temperature, and



with a dissociative recombination rate  $k_e = 5.2 \times 10^{-8} \times (T/300)^{-0.8} \text{ cm}^3 \text{ s}^{-1}$ . There, other destruction reactions with negative ions are neglected. By assuming steady state for the CF<sup>+</sup> abundance, the following relation is obtained:

$$\frac{[\text{CF}^+]}{[\text{HF}]} = \frac{k_f[\text{C}^+]}{k_e[e]} \approx \frac{k_f}{k_e} = 0.138 \times \left(\frac{T}{300}\right)^{0.65}, \quad (3)$$

where the electron density  $[e]$  is assumed to be roughly equal to the C<sup>+</sup> abundance in diffuse cloud. The recombination rate constant  $k_e$  has been measured by using a laboratory storage ring experiment (Novotny et al. 2005). On the other hand, the  $k_f$  value has not yet been measured. Neufeld et al. (2005) estimated the value via a statistical adiabatic capture model. Therefore, the coefficient 0.138 may have an uncertainty of a factor of 2–3. When we assume a kinetic temperature  $T = 100 \text{ K}$ , Eq. (3) gives the ratio  $[\text{CF}^+]/[\text{HF}]$  of  $\sim 7\%$ , where the  $T$  value corresponds to roughly  $A_V = 2$  from Fig. 10 of Nagy et al. (2013). In more sophisticated calculations, the ratio changes depending on the  $A_V$  value, taking the maximum ratio of  $\sim 10\%$  at  $A_V = 1$ , as shown in Fig. 3 of Neufeld & Wolfire (2009). From the observational point of view, the CF<sup>+</sup> abundance is thought to be about 1% of the gas-phase fluorine abundance in the Galactic diffuse clouds (e.g., Nagy et al. 2013).

CF<sup>+</sup> and HF were both detected toward the Galactic source W49 (Liszt et al. 2015), and the abundance ratio  $[\text{CF}^+]/[\text{HF}]$  is in the range 0.010–0.025 for various velocity components. The values are consistent if we consider the uncertainty of the calculated  $k_f$  (see also the discussion by Liszt et al. 2015) and the variations of C<sup>+</sup> abundance in diffuse clouds.

For the absorber toward PKS 1830–211, the HF  $J = 1-0$  line, redshifted into the ALMA band 9, has recently been detected (Kawaguchi et al. 2016) and shows a heavily saturated absorption toward the SW image with a HF column density  $> 3.4 \times 10^{14} \text{ cm}^{-2}$ . The fluoronium ion, H<sub>2</sub>F<sup>+</sup>, on the other hand, was not detected down to an abundance ratio  $[\text{H}_2\text{F}^+]/[\text{HF}] \leq 1/386$  ( $3\sigma$ ). This confirms that HF is the main molecular reservoir of fluorine.

## 4. Summary and conclusions

We report the detection of CF<sup>+</sup> in the  $z = 0.89$  absorber toward PKS 1830–211. This is the first extragalactic detection of this ion which, by now, has been observed in various Galactic sources. We find that the absorption line profile of CF<sup>+</sup> is significantly different from those of other species observed in the same tuning and is especially anticorrelated with CH<sub>3</sub>OH. We estimate a CF<sup>+</sup> fractional abundance of  $\sim 3 \times 10^{-10}$ , implying that only  $\sim 1\%$  of the interstellar fluorine is captured in this ion and that HF is by far the main reservoir of interstellar fluorine in the molecular phase.

*Acknowledgements.* This paper makes use of the following ALMA data: ADS/JAO.ALMA#2013.1.01099.S and ADS/JAO.ALMA#2011.0.00405.S. ALMA is a partnership of ESO (representing its member states), NSF (USA) and NINS (Japan), together with NRC (Canada) and NSC and ASIAA (Taiwan) and KASI (Republic of Korea), in cooperation with the Republic of Chile. The Joint ALMA Observatory is operated by ESO, AUI/NRAO, and NAOJ.

## References

- Asplund, M., Grevesse, N., Sauval, A. J., & Scott, P. 2009, *ARA&A*, 47, 481
- Fechtenbaum, S., Bontemps, S., Schneider, N., et al. 2015, *A&A*, 574, L4
- Guzmán, V., Roueff, E., Gauss, J., et al. 2012, *A&A*, 548, A94
- Kanekar, N., Ubachs, W., Menten, K. M., et al. 2015, *MNRAS*, 448, 104
- Kawaguchi, K., Muller, S., Black, J. H., et al. 2016, *ApJ*, in press
- Liszt, H. S., Pety, J., Gerin, M., & Lucas, R. 2014, *A&A*, 564, A64
- Liszt, H. S., Guzmán, V., Pety, J., Gerin, M., Neufeld, D. A., & Gratier, P. 2015, *A&A*, 579, A12
- Martí-Vidal, I., Vlemmings, W., Muller, S., & Casey, S. 2014, *A&A*, 563, A136
- Muller, S., & Guélin, M. 2008, *A&A*, 491, 739
- Muller, S., Beelen, A., Guélin, M., et al. 2011, *A&A*, 535, A103
- Muller, S., Beelen, A., Black, J. H., et al. 2013, *A&A*, 551, A109
- Muller, S., Combes, F., Guélin, M., et al. 2014a, *A&A*, 566, A112
- Muller, S., Black, J. H., Guélin, M., et al. 2014b, *A&A*, 566, L6
- Müller, H. S. P., Thorwirth, S., Roth, D. A., & Winnewisser, G. 2001, *A&A*, 370, L49
- Nagy, Z., Van der Tak, F. F. S., Ossenkopf, V., et al. 2013, *A&A*, 550, A96
- Neufeld, D. A., & Wolfire, M. G. 2009, *ApJ*, 706, 1594
- Neufeld, D. A., Wolfire, M. G., & Schilke, P. 2005, *ApJ*, 628, 260
- Neufeld, D. A., Schilke, P., Menten, K. M., et al. 2006, *A&A*, 454, 37
- Novotny, O., Mitchell, J. B. A., LeGarrec, J. L., et al. 2005, *J. Phys. B: At. Mol. Opt. Phys.*, 38, 1471
- Schulz, A., Henkel, C., Menten, K. M., et al. 2015, *A&A*, 574, A108
- Snow, T. P., Destree, J. D., & Jensen, A. G. 2007, *ApJ*, 655, 285
- Wiklind, T., & Combes, F. 1996, *Nature*, 379, 139
- Winn, J. N., Kochanek, C. S., McLeod, B. A., et al. 2002, *ApJ*, 575, 103

## Appendix A: Data

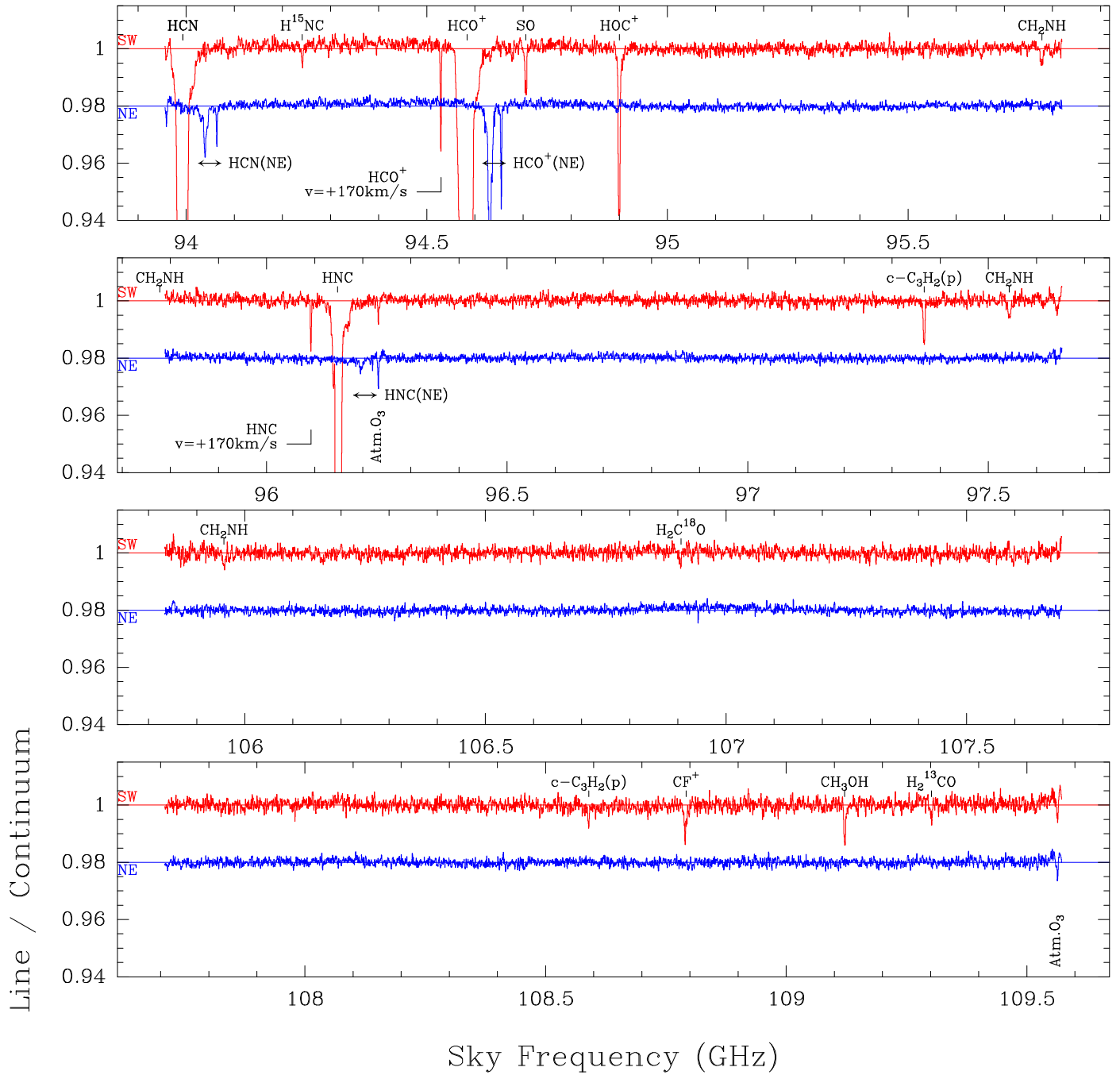


**Fig. A.1.** Full ALMA spectra toward the SW (in red) and NE (in blue, offset by  $-0.02$ ) images of PKS 1830–211. The spectra are normalized to the continuum level.